Density-functional theory for inhomogeneous electrolytes

R. D. Groot*
Research Institute for Metals, Laboratory of Solid State Chemistry, University of Nijmegen, Toernooiveld, 6525 ED Nijmegen, The Netherlands
(Received 26 October 1987)

A density-functional theory is developed in which the local density of a ionic fluid near an interface can be calculated. To find this local fluid structure, the Helmholz free energy is approximated using a perturbation expansion around an optimized reference state. The density of this reference state follows directly from the theory once an approximation for the direct correlation function in the homogeneous reference state is given; i.e., no coarse-graining procedure has to be imposed beforehand. Using the mean-spherical-approximation to the direct correlation function, the theory is applied to three different physical situations. In the restricted primitive electrolyte model near a charged wall we find layering of the counterions, and on adding a neutral third component we find spontaneous charge inversion; i.e., a negatively charged wall develops a positive potential. In the molten-salt regime the model shows very strong oscillations in the potential as a function of the distance from the wall, due to the fluctuation corrections.

I. INTRODUCTION

Although the electrostatic interaction is of dominant importance in many physical and chemical systems of interest, its influence in problems concerned with inhomogeneous fluids is still far from understood. The statistical mechanics of bulk electrolytes has been well established over the past decades, where most attention has been paid to the restricted primitive model (RPM).[1] Some cornerstones in this development are the analytic solutions of the mean-spherical approximation (MSA) of the neutral electrolyte by Waisman,[2] and of the one-component plasma by Palmer and Weeks.[3] Another important result is the derivation of the zeroth- and second-moment conditions by Stillinger and Lovett.[4]

For inhomogeneous fluids, i.e., fluids near a crystal surface or near a polymer, the latter moment conditions have recently been generalized by Carnie,[5] and a surface sum rule valid in the absence of mirror-image effects has been given by Henderson, Blum, and Lebowitz.[6] A first model for the electrostatic double layer that can be solved analytically has been developed by Gouy[7] and Chapman.[8] The model describes the local densities of a fluid of point charges near a charged wall. Its results for the density profiles and the potential drop over the double layer is reasonable if the charge density at the wall is low and if the ionic strength is low. If, however, the ions are modeled by an additional hard-sphere repulsion, and, moreover, if the surface charge increases, its predictions become qualitatively wrong, as has been shown in several simulation studies in flat[9-11] and cylindrical symmetry.[12-14]

Under these conditions the fluid builds up a second layer near the wall, which also cannot be described by the pure hypernetted-chain (HNC) theory or the modified Poisson-Boltzmann equation.[10] A review of the theory up to this point has been given by Carnie and Torrie.[15] Very recently some models have been developed that can account for this layering,[11,16-18] but for various reasons they cannot be used to describe a related problem in which the system parameters are different. This is the case as some authors optimize their model to meet the simulation results, and because others use an expansion for the bridge function, of which the validity at higher density is unknown.

As pointed out previously, only little information concerning inhomogeneous liquids is known exactly. In the absence of exact results, it is desirable to have a model, based on the least possible number of *ad hoc* assumptions or free parameters, as such a model would have a predictive value. The development of this model is the subject of the present article. The model is outlined in Secs. II and III, and an analysis of the effect of the electrostatic fluctuation corrections is given in Sec. IV. In Sec. V we apply the theory to the RPM near a charged wall, to a three-component electrolyte solution model, and to a simple model of a fused salt near an interface. In Sec. VI a brief summary of the model and the obtained qualitative results are given.

II. THE DENSITY-FUNCTIONAL METHOD

Throughout this article we shall consider an ensemble of particles that interact with the simplest possible pair potential to describe electrolytes. The repulsive part of the potential is taken to be a hard-sphere interaction, where all particles have the same diameter R. The different components are distinguishable from each other, as the charges differ. Explicitly, we take

$$V_{ij}(r)=\infty \quad \text{if } r<R \ ,$$
$$V_{ij}(r)=\frac{1}{4\pi\epsilon}\frac{q_i q_j}{r} \quad \text{if } r>R \ , \tag{1}$$

where ϵ is the dielectric constant of the medium. Note that we use the SI convention to describe the potential,

and not the rationalized Gauss convention.

In the grand canonical ensemble all equilibrium properties of the system can be calculated if the grand partition function is known. It can formally be written as

$$Z=\int \mathcal{D}\rho \exp(-\beta\Omega[\rho]) , \tag{2}$$

where $\int \mathcal{D}\rho$ stands for an integration over all possible configurations, and where Ω by definition is the grand potential (density) functional. From Eq. (2) it becomes clear that, since Ω is an extensive function, the most important contribution to Z comes from a region in function space, near the absolute minimum of Ω. Only near a critical point this minimum becomes very broad; we shall not consider this case here. Away from these points a mean-field description leads to a very reasonable approximation. Within such a scheme, only the absolute minimum of Ω is calculated, which can be done if an approximate expression for Ω in terms of the statistically averaged density at each point of space is known. In the remaining part of this section, we shall define such an approximate expression.

Our starting point is the definition of the n-point direct correlation functions,

$$\beta\frac{\delta^n(F[\rho]-F^{\mathrm{id}}[\rho])}{\delta\rho(x_1)\cdots\delta\rho(x_n)}=-C_n(x_1,\ldots,x_n) , \tag{3}$$

where $F=\Omega+\sum_i\mu_i\int\rho_i(r)d^3r$ is the Helmholz free-energy functional, and where F^{id} is the ideal-gas contribution to F. The parameters μ_i are externally given parameters. As we search for the minimum of Ω, these μ's can be identified with the chemical potentials of the various components. If the fluid is homogeneous $[\rho_i(x)=\bar\rho_i]$, their values are known from the theory of uniform fluids, and subsequently one may express the chemical potential of the nonuniform fluid as[19–21]

$$\begin{aligned}\beta\mu_i[\rho;\bar\rho](\mathbf{r})=&\ln[\rho_i(\mathbf{r})\lambda_i^3]+\beta\Delta\mu_i(\bar\rho(\mathbf{r}))\\&-\sum_j\int[C_2(\mathbf{r},\mathbf{r}';\bar\rho(\mathbf{r}))]_{ij}\\&\times[\rho_j(\mathbf{r}')-\bar\rho_j(\mathbf{r})]d^3r'+\cdots ,\end{aligned} \tag{4}$$

where $\Delta\mu(\bar\rho)$ is the excess chemical potential of a homogeneous fluid at density $\bar\rho$, and where λ_i is the thermal wavelength of particle type i.

The free energy per particle of type i can subsequently be found from integrating the chemical potential with respect to the density in the following manner:

$$\begin{aligned}\beta f_i[\rho,\bar\rho](\mathbf{r})=&\int_0^1\beta\mu_i[\zeta\bar\rho](\mathbf{r})d\zeta\\=&\ln[\rho_i(\mathbf{r})\lambda_i^3]-1+\beta\Delta f_i(\bar\rho)\\&-\sum_j\int G_{ij}(\mathbf{r}-\mathbf{r}';\bar\rho(\mathbf{r}))[\rho_j(\mathbf{r}')-\bar\rho_j(\mathbf{r})]d^3r' .\end{aligned} \tag{5}$$

If the series in (4) that contains all n-point functions is truncated after the C_2 term, Eq. (5) follows, in which

$$G_{ij}(\mathbf{r}-\mathbf{r}';\bar\rho(\mathbf{r}))=\int_0^1\zeta\,d\zeta\,C_{ij}(\mathbf{r}-\mathbf{r}';\zeta\bar\rho(\mathbf{r})) . \tag{6}$$

It has been shown[21] that the approximation to the free energy, given in Eq. (5), has an internal inconsistency, that results from truncating the series in (4). As a result of this truncation, Eq. (3) is not satisfied for $n=2$. When the given model is applied to the hard-sphere system, and the exact[22] hard-sphere direct correlation function is substituted into Eq. (6), the density-functional model leads to erroneous results, due to this truncation. To correct for this error, one may calculate an effective (renormalized) coupling G, such that Eq. (3) is satisfied up to $n=2$.[23] The resulting coupling function has developed a large tail for $r>1$, and it is observed that for the hard-sphere system at high density, the following function is a reasonable approximation to this renormalized coupling:

$$\begin{aligned}G(r)=&G^{\mathrm{PY}}(r)+E(r)\\=&G^{\mathrm{PY}}(r)+\frac{\pi}{6}\Theta(r-1)\frac{\eta^2}{(1-\eta)^3}\frac{e^{2\pi-2\pi r}}{r}\cos(2\pi r) ,\end{aligned} \tag{7}$$

where G^{PY} is the coupling that results from substituting the Percus-Yevic direct correlation function into Eq. (6), and where the hard-sphere diameter is used as a unit of length. Apparently the addition of the function $E(r)$ in Eq. (7) is a workable approximation to the series of higher-order n-point functions that sums up to the bridge function. Replacing this sum by the introduction of $E(r)$ thus leads to better results than a crude truncation does. The quality of the approximation, however, depends on the geometry of the problem, and of the actual packing fraction.

To introduce the electrostatic free-energy functional, we shall concentrate on a two-component mixture, for didactical reasons. Once the free energy of this problem has been formulated, the generalization to an arbitrary mixture is straightforward. The direct correlation functions of this problem may in general be written as

$$\begin{aligned}C_{++}(r)=C_{--}(r)=C_S(r)+C_D(r) ,\\C_{+-}(r)=C_{-+}(r)=C_S(r)-C_D(r) .\end{aligned} \tag{8}$$

Without loss of generality, the "difference" C_2 may be written as

$$C_D(r)=-\frac{\beta q^2}{4\pi\epsilon Rk_BT}\frac{1}{r}+\delta C_D(r) , \tag{9}$$

where again r is expressed in units of R. Henceforth we shall use the dimensionless charge $Q=q(\epsilon Rk_BT)^{-1/2}$, and the hard-sphere diameter as unit of length. The first term at the right-hand side of Eq. (9) represents the bare electrostatic potential. Because of the long-ranged nature of this term, it will be treated separately from the second term, which is of short range, and results from the fluctuation corrections. To describe the $1/r$ part of C_D, we introduce the internal electrostatic field, defined as the solution of the Laplace equation,

$$\Delta\phi^{\rm int}=-Q(\rho_+-\rho_-)\ , \tag{10}$$

where ρ_+ and ρ_- are the densities of the positively and negatively charged particles, respectively. The short-range part of the direct correlation function is to be taken into account by the introduction of a nonlocal coupling into the free-energy functional.

To find these coupling functions from the direct correlation functions, some care must be taken. It is straightforward to find the coupling functions from Eq. (6). However, this equation results from the approximate expression given in Eq. (4); therefore, it leads to erroneous results. Indeed, the analysis of the position of the poles of $\tilde{h}_D(k)$ in the complex k plane leads to the conclusion that, in the MSA approximation,[2] $h_D(r)$ is a damped monotonic function if the screening parameter $x=Q/\sqrt{\rho}<1.23$, a damped oscillating function for intermediate x, and an undamped oscillating function for $x\to x_d=\infty$. In the present model, the free energy is fully determined by the coupling G. As not all n-point functions are accounted for, the second variation of the excess free-energy functional does not equal the input direct correlation function in the approximation scheme given by Eq. (6). Now if in the linearized model that follows from this approximation to the couplings the pole structure of $\tilde{h}_D(k)$ is analyzed, one finds $h_D(r)$ to be undamped oscillating already at the finite value of the screening parameter $x_d=15.7$. For larger values of the screening parameter, the fluid state becomes unstable, and hence the system must freeze. The above mechanism must, however, not be seen as a valid theory of freezing, but merely as an artifact of the approximation scheme used to calculate the nonlocal coupling. Hence Eq. (6) may not be used to find the coupling functions.

Instead of using the approximate expression for the chemical potential, one should use the exact relations, given by Eq. (3) up to $n=2$, as defining conditions for the couplings. To relax these (exact) requirements, we shall use a perturbation expansion around the hard-sphere system, and thus take

$$G_S(r;\bar{\rho})=E(r;\bar{\rho})+\int_0^1 C_S(r;\zeta\bar{\rho})\zeta\,d\zeta\ , \tag{11a}$$

$$G_D(r;\bar{\rho})=\tfrac{1}{2}\delta C_D(r;\zeta\bar{\rho})\ . \tag{11b}$$

Note that G_D has no direct thermodynamic relevance, in the sense that the pressure of the system, found from the compressibility equation, is determined only by C_S. Therefore, Eq. (11b) is not in conflict with the compressibility equation.

The final step to find the free-energy functional makes use of the compressibility equation, which leads to the following relevant expressions for the excess free energy per particle:

$$\Delta f_S(\bar{\rho})=-(\bar{\rho}_++\bar{\rho}_-)\int_0^1 d\zeta\int d^3r\,G_S(\zeta\bar{\rho})\ , \tag{12a}$$

$$\Delta f_D(\bar{\rho})=-(\bar{\rho}_+-\bar{\rho}_-)\int_0^1 d\zeta\int d^3r\,G_D(\zeta\bar{\rho})\ . \tag{12b}$$

The combination of Eq. (5) and Eqs. (10)–(12) now leads to the following free energy of a fluid in an external field $\phi^{\rm ext}$:

$$\begin{aligned}\beta F[\rho,\bar{\rho}]=&\int d^3r\{\rho_+(\mathbf{r})\ln[\rho_+(\mathbf{r})\lambda_+^3]-\rho_+(\mathbf{r})+\rho_-(\mathbf{r})\ln[\rho_-(\mathbf{r})\lambda_-^3]-\rho_-(\mathbf{r})\\&+[\rho_+(\mathbf{r})+\rho_-(\mathbf{r})]\Delta f_S(\bar{\rho})+[\rho_+(\mathbf{r})-\rho_-(\mathbf{r})]\Delta f_D(\bar{\rho})+Q[\rho_+(\mathbf{r})-\rho_-(\mathbf{r})][\phi^{\rm ext}(\mathbf{r})+\tfrac{1}{2}\phi^{\rm int}(\mathbf{r})]\}\\&+\int d^3r\,d^3r'\begin{bmatrix}\rho_+(\mathbf{r})\\ \rho_-(\mathbf{r})\end{bmatrix}\begin{bmatrix}G_S(\mathbf{r}-\mathbf{r}')+G_D(\mathbf{r}-\mathbf{r}') & G_S(\mathbf{r}-\mathbf{r}')-G_D(\mathbf{r}-\mathbf{r}')\\ G_S(\mathbf{r}-\mathbf{r}')-G_D(\mathbf{r}-\mathbf{r}') & G_S(\mathbf{r}-\mathbf{r}')+G_D(\mathbf{r}-\mathbf{r}')\end{bmatrix}\begin{bmatrix}\rho_+(\mathbf{r}')-\bar{\rho}_+(\mathbf{r})\\ \rho_-(\mathbf{r}')-\bar{\rho}_-(\mathbf{r})\end{bmatrix}\ ,\end{aligned} \tag{13}$$

where $\phi^{\rm ext}(\mathbf{r})$ is a density-independent field, due to external sources, and where $\phi^{\rm int}(\mathbf{r})$ is the solution of Eq. (10). Hence it is proportional to $\rho_+-\rho_-$ and therefore its prefactor $\frac{1}{2}$ appears in the free energy.

One may now define three electrostatic potentials.[15] Firstly, the field $\phi^{\rm ext}$ is the field that a test particle would "feel" if no fluid were present. Secondly, due to the presence of the charged fluid, an infinitesimal point charge would feel the local potential,

$$\psi(\mathbf{r})=\phi^{\rm ext}(\mathbf{r})+\phi^{\rm int}(\mathbf{r})\ , \tag{14}$$

and finally, the electrostatic potential of mean force must be defined as the variation of the free energy with respect to the local charge density,

$$\phi^{\rm MF}(\mathbf{r})=\frac{1}{Q}\frac{\delta F[\rho,\bar{\rho}]}{\delta(\rho_+(\mathbf{r})-\rho_-(\mathbf{r}))}\ , \tag{15}$$

which is the effective potential that a fluid particle feels. In general, this is a rather complicated expression, being the sum of the local potential $\psi(\mathbf{r})$ and the fluctuation potential. The latter is determined by the difference coupling function, hence in practice it is directly influenced by the approximations used for the couplings. For simplicity, we shall therefore study $\psi(\mathbf{r})$ and compare this quantity with the simulation results for $\psi(\mathbf{r})$.

III. FIELD EQUATIONS AND REFERENCE DENSITIES

The field equations that lead to the minimization of the grand potential

$$\Omega[\rho,\bar{\rho}]=F[\rho,\bar{\rho}]-\sum_i\mu_i\int\rho_i(\mathbf{r})d^3r \tag{16}$$

can readily be found from Eq. (13). As Ω is a functional of both ρ and $\bar{\rho}$, two types of equations are involved. The

first type expresses local chemical equilibrium, and follows from

$$\frac{\delta\Omega[\rho,\bar{\rho}]}{\delta\rho_i(\mathbf{r})}=0 \tag{17}$$

for each component. The requirement that the free energy also be stationary with respect to the reference density, i.e.,

$$\frac{\delta\Omega[\rho,\bar{\rho}]}{\delta\bar{\rho}_i(\mathbf{r})}=0\ , \tag{18}$$

directly leads to an expression of $\bar{\rho}(r)$ in terms of a functional of the density $\rho(r)$.

To continue, we need a model for the direct correlation functions. In any model that uses a neutral reference state, the sum and difference direct correlation functions both are functions of the sum of the particle densities; examples are the MSA (Ref. 2) and the GMSA (generalized mean-spherical approximation) (Ref. 24) approximations. This implies that Eq. (18) leads to the same condition on variation with respect to $\bar{\rho}_+$ and on variation with respect to $\bar{\rho}_-$. Apart from some cancellations, one finds upon variation,

$$\begin{bmatrix}\rho_+(\mathbf{r})\\ \rho_-(\mathbf{r})\end{bmatrix}\int d^3r'\begin{bmatrix}G_S'+G_D' & G_S'-G_D'\\ G_S'-G_D' & G_S'+G_d'\end{bmatrix}\times\begin{bmatrix}\rho_+(\mathbf{r}')-\bar{\rho}_+(\mathbf{r})\\ \rho_-(\mathbf{r}')-\bar{\rho}_-(\mathbf{r})\end{bmatrix}=0\ , \tag{19}$$

where $G_{S,D}'$ stands for $\partial G_{S,D}(\mathbf{r}-\mathbf{r}';\bar{\rho})/\partial(\bar{\rho}_+ +\bar{\rho}_-)$.

On a local scale, $\rho_+(\mathbf{r})$ and $\rho_-(\mathbf{r})$ may in practice have quite large variations, whereas the reference densities, which are *a priori* independent from the former ones, should vary slowly. This only is manifest if we impose the stronger condition

$$\int d^3r'\begin{bmatrix}G_S'+G_D' & G_S'-G_D'\\ G_S'-G_D' & G_S'+G_D'\end{bmatrix}\begin{bmatrix}\rho_+(\mathbf{r}')-\bar{\rho}_+(\mathbf{r})\\ \rho_-(\mathbf{r}')-\bar{\rho}_-(\mathbf{r})\end{bmatrix}=\begin{bmatrix}0\\0\end{bmatrix}\ . \tag{20}$$

This requirement can be worked out to find the sum and difference of the reference densities,

$$\bar{\rho}_+(\mathbf{r})+\bar{\rho}_-(\mathbf{r})=\frac{\int G_S'[\rho_+(\mathbf{r}')+\rho_-(\mathbf{r}')]d^3r'}{\int G_S'd^3r}\ , \tag{21a}$$

$$\bar{\rho}_+(\mathbf{r})-\bar{\rho}_-(\mathbf{r})=\frac{\int G_D'[\rho_+(\mathbf{r}')-\rho_-(\mathbf{r}')]d^3r'}{\int G_D'd^3r'}\ . \tag{21b}$$

Hence the sum-reference density is an average over the sum of the local densities, weighed by the derivative of the sum coupling, and an analogous relation holds for the difference-reference density. One thus finds the reference densities in a quite natural manner. This way the model gains much in predictive capacity. It should at this point be stressed that we were forced to impose the stronger condition (20) rather than (19), only because the direct correlation function of a neutral reference state contains no explicit dependence on the difference of the particle densities. If, however, a non-neutral electrolyte[25] is used as a reference, as is done in Ref. 16, then the given postulate is not necessary, hence the theory would then become fully self-contained.

The field equations for the local densities can finally be expressed as

$$\begin{aligned}\beta\mu_\pm=&\ln[\rho_\pm(\mathbf{r})\lambda_\pm^3]+[\bar{\rho}_+(\mathbf{r})+\bar{\rho}_-(\mathbf{r})]\left[G_S(\bar{\rho})-\int_0^1 d\zeta\, G_S(\zeta\bar{\rho})\right]\\ &\pm[\bar{\rho}_+(\mathbf{r})-\bar{\rho}_-(\mathbf{r})]\left[G_D(\bar{\rho})-\int_0^1 d\zeta\, G_D(\zeta\bar{\rho})\right]\pm Q[\phi^{\rm ext}(\mathbf{r})+\phi^{\rm int}(\mathbf{r})]\\ &-\int d^3r'[\rho_+(\mathbf{r}')+\rho_-(\mathbf{r}')][G_S(\mathbf{r}-\mathbf{r}';\bar{\rho}(\mathbf{r}))+G_S(\mathbf{r}-\mathbf{r}';\bar{\rho}(\mathbf{r}'))]\\ &\mp\int d^3r'[\rho_+(\mathbf{r}')-\rho_-(\mathbf{r}')][G_D(\mathbf{r}-\mathbf{r}';\bar{\rho}(\mathbf{r}))+G_D(\mathbf{r}-\mathbf{r}';\bar{\rho}(\mathbf{r}'))]\ ,\end{aligned} \tag{22}$$

where we have used the shorthand notation $G(\bar{\rho})$ for $\int d^3r'G(\mathbf{r}-\mathbf{r}';\bar{\rho}_+(\mathbf{r})+\bar{\rho}_-(\mathbf{r}))$. Note that the internal electrostatic field has a prefactor 1 in the chemical potential, as it by definition equals the solution of Eq. (10), and thus is proportional to the density itself.

IV. ELECTROSTATIC FLUCTUATION CORRECTIONS

To gain insight in the nature of the electrostatic fluctuation correction that gives rise to the fluctuation potential, we have studied a series of models that characterize the effect. The simplest possible model is found if one puts

$$\delta C_D(r)=0 \tag{23}$$

in Eq. (9). The resulting model will be denoted by "mean field," as it contains only the bare electrostatic interaction. It does, however, describe the hard-sphere interaction quite satisfactorily, hence the resulting field equations may be interpreted as a Poisson-Boltzmann equation, modified for the hard-sphere effects.

The simplest model that does account for the mutual rearrangements of the fluid particles can be found if the lowest-order hard-sphere interaction is taken into account. Due to this repulsion, there is no pair of particles closer to each other than the hard-sphere diameter. Hence the electrostatic potential only contributes to the

free energy outside of a spherical cavity with unit radius. This means that the difference direct correlation function to lowest approximation is given by

$$C_D(r)=-\frac{Q^2}{4\pi r}\Theta(r-1)=-\frac{Q^2}{4\pi r}+\delta C_D(r)\ , \tag{24}$$

hence $\delta C_D(r)=Q^2/4\pi r$ if $r<1$, and it vanishes otherwise. We shall call this the cavity approximation. Note that in this approximation the third term in Eq. (22) vanishes; therefore, one need not determine the difference-reference density.

A less trivial, but still analytically tractable, approximation is the MSA. It is found from solving the Ornstein-Zernike equation

$$h_D(r)=C_D(r)+\bar{\rho}\,C_D^* h_D(r)\ , \tag{25}$$

under the conditions

$$C_D(r)=-\frac{Q^2}{4\pi r}\quad \text{if } r>1\ , \tag{26a}$$

$$h_D(r)=0\quad \text{if } r<1\ , \tag{26b}$$

where $h_D=(h_{++}-h_{+-})/2$, $\bar{\rho}=\bar{\rho}_+ +\bar{\rho}_-$, and where $*$ stands for a spatial convolution. From Eq. (25), C_D may be solved analytically[2] for $r<1$, and h_D may be solved[26] for $r>1$. The result for the direct correlation can be written as

$$\delta C_D(r)=\frac{Q^2}{4\pi r}(1-Br)^2\Theta(1-r)\ , \tag{27}$$

where $B=(1+x-\sqrt{1+2x})/x$ and $x=Q\sqrt{\bar{\rho}}$ is the Debye-Huckel screening parameter. Indeed, at low density $B\approx 0$, and (27) approaches our simple cavity approximation (24). One may consider the fluctuation correction to be an effective potential, which must be added to the bare potential, but which has opposite sign. It thus corrects for "overcounting" the potential, which happens in the mean-field approximation. The value of this overcounting is underestimated in the mean-field approximation (as it is put equal to zero), but it is overestimated in the cavity approximation, as will be shown in the following.

We have chosen to compare these models in an extreme situation, for which simulation results are available. For each model we have calculated the density profiles near a charged wall in the RPM electrolyte model defined by Eq. (1). The parameters chosen are diameter $R=4.25$ Å, temperature $T=298$ K, relative dielectric constant $\epsilon_r=78.5$, and the bulk density $\bar{\rho}=\bar{\rho}_+ +\bar{\rho}_-=0.0924$, which at the given particle diameter equals 1 mol/l. The charge density at the wall has been fixed at $\sigma^*=\sigma R^2/q=0.70$. According to Torrie and Valleau,[10] the potential drop over the double layer, i.e., the potential at distance $R/2$ from the wall, equals 147±4 mV in this problem. More recently, Ballone *et al.*[11] have reported a potential drop of 132 mV. Both values result from simulations; the cause of this variance is at present unclear.

The density profiles that result from the three different models have been plotted in Fig. 1. The mean-field model

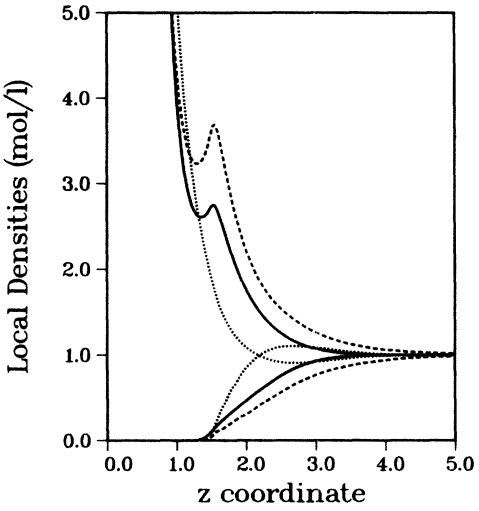

FIG. 1. Density profiles in the RPM near a charged wall, resulting from the mean-field model (dashed curves), the cavity approximation (dotted curves), and the MSA approximation (solid curves) for C_D.

shows a strong tendency to form a layered structure, just as the simulation results do. The potential drop in this model, however, is 183 mV, which must be considered to be too large. In the cavity model, this layering has disappeared, which can be understood from the fact that the fluctuation potential acts as an attractive potential between particles of the same sign. It is therefore favorable for the system to concentrate all countercharge in a single thin layer. This small thickness of the double layer causes the potential drop to be significantly smaller than in the mean-field model; its value is 71 mV, which is an underestimate relative to the simulation result.

The density profiles and the potential drop in the MSA based model are somewhere intermediate between the former two models; we find a potential drop of 122 mV, which is some 7% below the result of Ballone *et al.* One possible cause of this deficiency may be the fact that our approximation to the bridge function is less satisfactory at these lower densities than it is at higher densities. Furthermore, the use of a non-neutral reference state[25] to calculate the fluctuation correction may improve the results of the present theory, as the resulting model would be self-contained with respect to the determination of the reference densities. Before doing so, one should, however, first rule out the simpler approximations.

V. SOME APPLICATIONS

The general theory described in the preceding sections may be applied to several problems. In the present article, we shall only summarize some of the possible applications, and give the qualitative results obtained in each situation. More detailed results are to be given in future publications on each subject.

The first problem considered is the restricted primitive model of electrolytes, defined as the two-component plas-

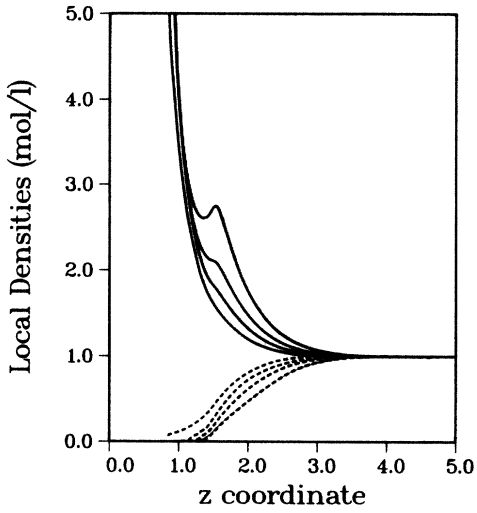

FIG. 2. Density profiles of counterions (solid curves) and coions (dashed curves) in the RPM near a charged wall, for the surface charge densities $\sigma^*=0.25$, 0.42, 0.55, and 0.70.

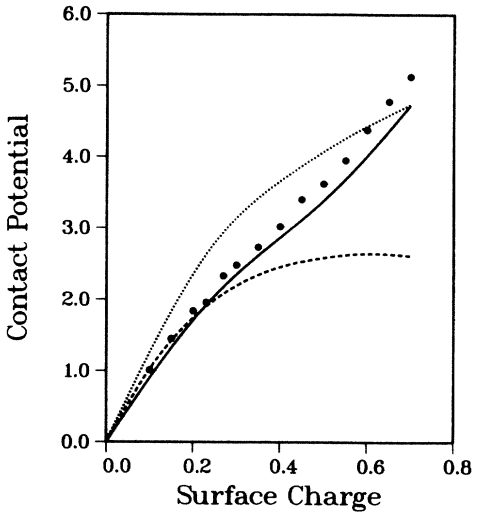

FIG. 3. The potential drop over the double layer as a function of the surface charge density, at 1 M, as resulting from the present theory (solid curve), from the HNC-MSA theory (dashed curve), and from the modified Gouy-Chapman equation (dotted curve). The dots are simulation results taken from Ref. 11.

ma, interacting through the potential given in Eq. (1). The parameters chosen have been given in Sec. IV. We study this fluid near a hard flat charged wall in the MSA-based model, for the surface charge densities $\sigma^*=0.25$, 0.42, 0.55, and for $\sigma^*=0.70$, at which simulation results are available. The density profiles for these situations have been plotted in Fig. 2. In Fig. 3 we have plotted the potential drop over the double layer, commonly expressed as $\psi^*=q\psi_{1/2}/k_BT$, which is the dimensionless field at half the hard-sphere diameter from the wall. For comparison, the (modified) Gouy-Chapman result, the HNC-MSA result, and the Monte Carlo results of Ballone *et al.*[11] have been given in the same figure. It is very remarkable to observe that the Gouy-Chapman model, in which all hard-sphere and fluctuation corrections are neglected, performs better than the pure HNC model, which predicts a divergent differential double-layer capacity.

To describe a real electrolyte solution, the RPM has an obvious shortcoming, as it does not describe the solvent explicitly. Since many of the structural properties of a fluid are caused by the repulsive interactions with all particles present, one may expect the absence or presence of a solvent to have a large influence on the resulting charge distribution. To describe a realistic fluid, solvent-solvent and ion-solvent attractions should also be taken into account, but it is instructive to see what happens if only the repulsive short-range part of the potential is introduced. We therefore suggest that one study a three-component mixture, interacting with the potential defined in Eq. (1), and being composed of particles having charges q, $-q$, and 0. To compare the results of this model with those of the RPM, we have taken the same parameters as for the former calculations, but we have chosen the density of the neutral component to equal $\bar{\rho}_3=0.80$.

In the MSA approximation, C_S is just the Percus-Yevic hard-sphere direct correlation function, i.e., $C_S=C_S(\bar{\rho}_1+\bar{\rho}_2+\bar{\rho}_3)$. The difference direct correlation function C_D, however, is only a function of the screening parameter $x^2=\sum_i Q_i^2\bar{\rho}_i=Q^2(\bar{\rho}_1+\bar{\rho}_2)$, hence $C_D=C_D(\bar{\rho}_1+\bar{\rho}_2)$. The linearity of the Ornstein-Zernike equation now implies that we have the following nonlocal coupling in this three-component case:

$$G_{ij}=\begin{bmatrix} G_S+G_D & G_S-G_D & G_S \\ G_S-G_D & G_S+G_D & G_S \\ G_S & G_S & G_S \end{bmatrix} . \tag{28}$$

A straightforward generalization of Eq. (21) now leads to

$$\bar{\rho}_1+\bar{\rho}_2+\bar{\rho}_3=\frac{\int G_S'(\mathbf{r}-\mathbf{r}';\bar{\rho}_1+\bar{\rho}_2+\bar{\rho}_3)[\rho_1(\mathbf{r}')+\rho_2(\mathbf{r}')+\rho_3(\mathbf{r}')]d^3r'}{\int G_S'(\mathbf{r}-\mathbf{r}';\bar{\rho}_1+\bar{\rho}_2+\bar{\rho}_3)d^3r'} , \tag{29a}$$

$$\bar{\rho}_1+\bar{\rho}_2=\frac{\int G_S'(\mathbf{r}-\mathbf{r}';\bar{\rho}_1+\bar{\rho}_2+\bar{\rho}_3)[\rho_1(\mathbf{r}')+\rho_2(\mathbf{r}')]d^3r'}{\int G_S'(\mathbf{r}-\mathbf{r}';\rho_1+\rho_2+\rho_3)d^3r'} , \tag{29b}$$

$$\bar{\rho}_1-\bar{\rho}_2=\frac{\int G_D'(\mathbf{r}-\mathbf{r}';\bar{\rho}_1+\bar{\rho}_2)[\rho_1(\mathbf{r}')-\rho_2(\mathbf{r}')]d^3r'}{\int G_D'(\mathbf{r}-\mathbf{r}';\bar{\rho}_1+\bar{\rho}_2)d^3r'} , \tag{29c}$$

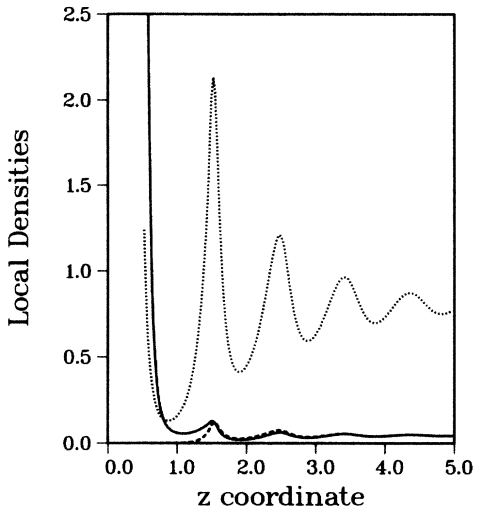

FIG. 4. Density profiles of counterions (solid curve), coions (dashed curve), and neutral particles (dotted curve), resulting from the electrolyte solution model.

where the reference densities are taken at the point r.

The density profiles for $\sigma^*=0.70$ have been plotted in Fig. 4, and in Fig. 5 the resulting potential is shown as a function of the distance from the wall for the various surface charges. Where in the RPM model the potential is a monotonous function of the distance from the wall, we find in this model a qualitatively different behavior. The system shows a spontaneous charge inversion, i.e., a positively charged wall produces a negative potential at some distance from the wall. Furthermore, we find a typical value of the potential (such as the depth of the minimum) to be an order of magnitude smaller than the potential drop in the RPM. A similar effect has been found if the model is used in cylindrical symmetry. One may expect this charge inversion to be caused by the poor solubility of an electrolyte in a strictly nonpolarizable solvent.

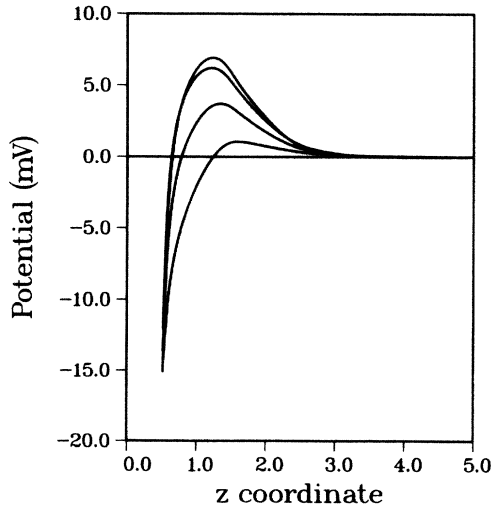

FIG. 5. Electrostatic potential in the electrolyte solution model; the surface charge densities are the same as for Fig. 2.

Finally, we mention calculations in the RPM to model a fused salt confined between two hard flat walls, for $\bar{\rho}=0.669$, at temperature $T=1500$ K. The particle diameter has been fixed at $R=3.14$ Å, and the value of ϵ_r has been varied. The surface charge at the left wall is varied from $\sigma^*=0.10$ to $\sigma^*=0.40$, for which Li and Mazo have performed calculations in the GMSA for the half infinite system.[27] The boundary condition at the right-hand side of the system is $\psi=0$ at the wall. The density profiles of the system with $\epsilon_r=2$ and $\sigma^*=0.40$ are given in Fig. 6. For these parameters the model shows a very strong layering of the fluid near the walls, and a large correlation length. The system furthermore shows oscillations in the charge density, which also are characteristic of a bulk molten salt,[28,29] thus implying oscillations in the potential $\psi(z)$.

In the present model one may define the thickness of the adsorbed layer to the wall (or the wall-particle correlation length), as the distance over which the amplitude of these oscillations decreases by a factor $1/e$. If the charge at the wall is small ($\sigma^*=0.10$), one thus finds a layer thickness that equals the MSA correlation length, within the accuracy by which the former ones could be obtained. As the charge at the wall increases, however, the thickness of the adsorbed becomes larger than the MSA correlation length, when the electrostatic coupling Q is large. For instance, we find a layer thickness of 3.3 at $\epsilon_r=2$ and $\sigma^*=0.40$, whereas the MSA correlation length equals $\xi=2.5$ at this coupling. One furthermore finds the wall to be "coated" by the salt: close to the wall, the sum-reference density is increased compared to the density in the bulk, over a considerable region (several hard-sphere diameters). For $\epsilon_r=1$ and $\sigma^*=0.40$ this density increase is over 3%.

VI. DISCUSSION

The model described in the preceding sections may be used as a tool to predict the thermodynamic and structural properties of inhomogeneous charged fluids. The model is a straightforward generalization of the re-

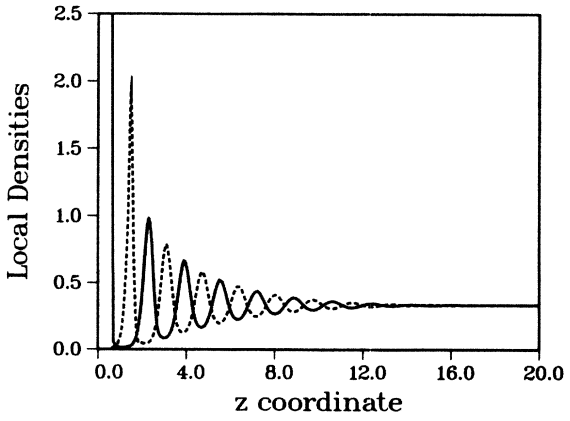

FIG. 6. Density profiles in the RPM of counterions (solid curve) and of coions (dashed curve) at typical fused salt conditions. The surface charge density equals $\sigma^*=0.40$.

normalized density-functional model published earlier.[22] It is based on an expression for the free energy, containing a local thermodynamic function and a (nonlocal) two-point coupling. To take the effect of the bridge function into account, the pure PY-based coupling has been modified by adding an oscillating tail. This approximation is valid at high density. The densities of the reference state, from which the perturbations are calculated, follow in a natural way from the theory. Once an approximation for the coupling function is chosen, the weight functions that determine the coarse-grained densities follow. This makes the theory self-contained: we did not have to put in by hand a weight function to fix the simulation results.

The latter implies that one can use the model to test several approximations for the direct correlation functions. Their influence on the potential drop in the electrostatic double layer may thus be studied systematically. As the lowest-order effect of the hard-sphere interaction is to push away all charge from the position where a particle is placed, this particle as a result feels a fluctuation potential, that has an opposite sign, relative to the bare interaction. This effect reduces the size of the double layer, and hence reduces the potential drop. It furthermore allows for the possibility of charge inversion near the wall.

The effect of charge inversion can be demonstrated easily, if a third (neutral) particle is added to the system, thus modeling an electrolyte solution. Due to the fluctuation corrections, the system may gain internal energy, if solvent particles from the first liquid layer adjacent to the wall are replaced by counterions. The cost in this case is only the ideal entropy of mixing, whereas in the RPM model (without the solvent) the cost of extra counterions is the excess free energy related to the hard-sphere repulsion.

As the density in the RPM is increased and the dielectric constant is decreased, one enters the region of fused salts. In this region a strong layering of the fluid near the walls is observed. The model that follows straightforwardly from the truncated expansion of the chemical potential in terms of n-point functions, shows an instability of the fluid phase at a finite temperature, which is not present in the MSA approximation. This implies that the truncated expansion may not be used in this parameter region, and a better approximation to define the coupling function is essential for a qualitatively correct description.

The model introduced here does not show this instability, but it does show an increased wall-particle correlation length at sufficiently high coupling and wall charge. It also shows a considerable increase in the local sum-reference density close to the wall, under these circumstances. Now the simulation results by Larsen, of the bulk correlation function at parameters that correspond to $\epsilon_r = 1$ in our notation, show the presence of extra peaks at $r = 2$ and 3 (see Fig. 2 in Ref. 27). These peaks are an indication of the presence of large clusters in the sample. Hence at $\epsilon_r = 1$ the system at least is close to solid-liquid coexistence. Our observed increase of the density near the wall, and the increasing thickness of the oscillating layer, may thus be interrelated in the following manner. As the system approaches the solid-liquid transition, the presence of the wall may pull the system away from the (stable) liquid phase into the (metastable) solid phase. We thus conjecture the wall to be coated by the solid phase, on the analogy of wetting phenomena at liquid vapor coexistence. The model can, however, not describe a real solid phase, as the density is averaged laterally. One may therefore expect only a qualitatively correct description: only the order of magnitude of the thickness of the adsorbed "solid" layer may be reproduced.

Hopefully the qualitative new results of the present theory will stimulate other authors to perform Monte Carlo or molecular-dynamics simulations on the systems described above. Apart from testing the present theory, these simulations would be of major importance to the understanding of a number of physical systems.

---

*Present address: Unilever Research Laboratorium, PAS, Surface Chemistry and Rheology, Postbox 114, 3130 AC Vlaardingen, The Netherlands.

[1]B. Hafkjold and G. Stell, in *The Liquid State of Matter: Fluids, Simple and Complex*, edited by E. W. Montroll and J. L. Lebowitz (North-Holland, Amsterdam, 1982).

[2]E. Waisman and J. L. Lebowitz, J. Chem. Phys. **52**, 4307 (1970).

[3]R. G. Palmer and J. D. Weeks, J. Chem. Phys. **58**, 4171 (1973).

[4]F. H. Stillinger and R. Lovett, J. Chem. Phys. **49**, 1991 (1968).

[5]S. L. Carnie, Chem. Phys. Lett. **77**, 437 (1981).

[6]D. Henderson, L. Blum, and J. L. Lebowitz, J. Electroanal. Chem. **102**, 315 (1979).

[7]G. Gouy, J. Phys. Radium **9**, 457 (1910).

[8]D. L. Chapman, Philos. Mag. **25**, 475 (1913).

[9]W. van Megen and I. Snook, J. Chem. Phys. **73**, 4656 (1980).

[10]G. M. Torrie and J. P. Valleau, J. Chem. Phys. **73**, 5807 (1980).

[11]P. Ballone, G. Pastore, and M. P. Tosi, J. Chem. Phys. **85**, 2943 (1986).

[12]D. Bratko and V. Vlachy, Chem. Phys. Lett. **90**, 434 (1982).

[13]M. Le Bret and B. H. Zimm, Biopolymers **23**, 271 (1984).

[14]V. Vlachy and A. D. J. Haymet, J. Chem. Phys. **84**, 5874 (1986).

[15]S. L. Carnie and G. M. Torrie, Adv. Chem. Phys. **4L**, 141 (1984).

[16]P. Nielaba and F. Forstmann, Chem. Phys. Lett. **117**, 46 (1985).

[17]R. Kjellander and S. Marcelja, Chem. Phys. Lett. **127**, 402 (1986).

[18]T. Alts, P. Nielaba, B. d'Aguanno, and F. Forstmann, Chem. Phys. **111**, 223 (1987).

[19]W. F. Saam and C. Ebner, Phys. Rev. A **15**, 2566 (1977).

[20]T. F. Meister and D. M. Kroll, Phys. Rev. A **31**, 4055 (1985).

[21]R. D. Groot, Mol. Phys. **60**, 45 (1987).

[22]R. D. Groot, J. P. van der Eerden, and N. M. Faber, J. Chem.

Phys. **87**, 2263 (1987).
[23]R. D. Groot and J. P. van der Eerden, Phys. Rev. A **36**, 4356 (1987).
[24]M. Parinello and M. P. Tosi, Chem. Phys. Lett. **64**, 579 (1979).
[25]D. Henderson and W. R. Smith, J. Stat. Phys. **19**, 191 (1978).
[26]S. Li and R. M. Mazo, J. Chem. Phys. **86**, 5757 (1987).
[27]B. Larsen, Chem. Phys. Lett. **27**, 47 (1974).
[28]L. V. Woodcock and K. Singer, Trans. Faraday Soc. **67**, 12 (1975).
[29]G. Stell and S. F. Sun, J. Chem. Phys. **63**, 5333 (1975).